Estimating wildfire-generated ozone over North America using ozonesonde profiles and a differential back trajectory technique

Omid Moeini [a,b,*], David W. Tarasick [b], C. Thomas McElroy [a], Jane Liu [c], Mohammed K. Osman [b], Anne M. Thompson [d], Mark Parrington [e], Paul I. Palmer [f], Bryan Johnson [g], Samuel J. Oltmans [g,h], John Merrill [i]

[a] Department of Earth and Space Science and Engineering, York University, Toronto, ON, Canada
[b] Air Quality Research Division, Environment and Climate Change Canada, Toronto, ON, Canada
[c] Department of Geography, University of Toronto, Toronto, ON, Canada
[d] NASA Goddard Space Flight Center, Greenbelt, MD, USA
[e] European Centre for Medium-Range Weather Forecasts, Reading, UK
[f] School of GeoSciences, The University of Edinburgh, UK
[g] NOAA Earth System Research Laboratory, Global Monitoring Division, Boulder, CO, USA
[h] Cooperative Institute for Research in Environmental Sciences, University of Colorado, Boulder, CO, USA
[i] Graduate School of Oceanography, University of Rhode Island, Narragansett, RI, USA

ARTICLE INFO

ABSTRACT

An objective method, employing HYSPLIT back-trajectories and Moderate Resolution Imaging Spectroradiometer (MODIS) fire observations, is developed to estimate ozone enhancement in air transported from regions of active forest fires at 18 ozone sounding sites located across North America. The Differential Back Trajectory (DBT) method compares mean differences between ozone concentrations associated with fire-affected and fire-unaffected parcels. It is applied to more than 1100 ozonesonde profiles collected from these sites during the summer months June to August 2006, 2008, 2010 and 2011. Layers of high ozone associated with low humidity were first removed from the ozonesonde profiles to minimize the potential effects of stratospheric intrusions on the calculations. No significant influence on average ozone levels by North American fires was found for stations located at Arctic latitudes. The ozone enhancement for stations nearer large fires, such as Trinidad Head and Bratt's Lake, was up to 4.8% of the TTOC (Total Tropospheric Ozone Column). Fire ozone accounted for up to 8.3% of TTOC at downwind sites such as Yarmouth, Sable Island, Narragansett, and Walsingham. The results are consistent with other studies that have reported an increase in ozone production with the age of the smoke plume.

1. Introduction

Tropospheric ozone (O_3) is an important regulated air pollutant. Exposure to elevated concentrations of ozone has been linked to respiratory illnesses such as asthma and is known to irritate lungs and aggravate bronchitis (Lippmann, 1991; McConnell et al., 2002; Bell et al., 2014; Szyszkowicz and Rowe, 2016). Ozone in the troposphere is formed by the interaction of nitrogen oxides ($NOx = NO + NO_2$), carbon monoxide (CO) and non-methane hydrocarbons (NMHCs) in the presence of sunlight, and is also transported from the stratosphere. Wildfires generate large amounts of such ozone precursors and a number of

studies suggest that fires can contribute to exceedance of the ozone air quality threshold concentrations via production and long-range transport of ozone and its photochemical precursors (Jaffe et al., 2004; Palmer et al., 2013; Parrington et al., 2013). In addition, the frequency and intensity of forest fires is likely to increase over Canada and the US as a result of climate change (Spracklen et al., 2009). Wotton et al. (2010) estimate an increase of 30% in boreal forest fire occurrence by 2030.

Ozone production from tropical biomass burning has been well established (Andreae and Merlet, 2001; Andreae et al., 1994; Jacob et al., 1996; Thompson et al., 1996; Thompson and Witte, 2001; Weller

---

et al., 1996). Both fuel consumption and the intensity of boreal fires are typically an order of magnitude larger than for savannah fires (Stocks et al., 1998). The higher intensity implies more vigorous transport of emissions, higher into the troposphere and even into the stratosphere (Fromm and Servranckx, 2003) which may lead to very long range transport. Data collected by aircraft, ground-based instruments and satellites during dozens of field investigations in recent decades over the Arctic and sub-Arctic have been used to study ozone production from boreal fires.

Different approaches and datasets used to address the ozone source issue appear to give conflicting results (Jaffe and Wigder, 2012). For instance, Olsen et al. (2012), using data collected by the DC-8 aircraft from summertime Arctic (ARCTAS-B) flights in central and eastern Arctic Canada (designated as $> 50^{o}$N latitude) to constrain a photo-chemical box model, found 1–2 ppbv/day net ozone photochemical formation in the boundary-layer (BL) and upper troposphere (UT), although with significant uncertainty due to uncertainties in measured NO and HOx. Alvarado et al. (2010) also used aircraft data obtained during the ARCTAS-B campaign to determine the enhancement ratio of reactive nitrogen (NOy) species from fresh plumes to examine the impact of these emissions on tropospheric ozone in the Arctic. The GEOS-Chem model showed very little ozone formation, mainly due to rapid conversion of NOx produced from fresh Arctic biomass burning to PAN and inorganic nitrates. In contrast, biomass burning from central Canada was found as a modest but significant source of ozone by Parrington et al. (2012). Like Alvarado et al. (2010), they used FLAMBE emissions for 2010 in GEOS-Chem, but the difference, as suggested by Parrington et al. (2013), seems to be that while fresh plumes (<2 days old) show little increase in ozone, in aged (>4 days) plumes PAN decomposition will release its constituent NO_2 and peroxy radicals which can then photolyze or react with NO to produce ozone. Furthermore, Finch et al. (2014) showed that the aerosol loading resulted from fire activity slows down the plume photochemistry. Busilacchio et al. (2016) used aircraft data collected during the Quantifying the impact of BOReal forest fires on Tropospheric oxidants using Aircraft and Satellites (BORTAS–B) campaign in 2011 to compare ozone and total peroxy nitrates (ΣPNs, ΣROONO2) production in fire plumes and background air masses. Using different approaches, (1) direct calculation and (2) 0-D photochemical model, the ozone and ΣPN formation in plumes impacted by fire emissions were compared with that in background air. They found that, on average, ΣPN production is more strongly enhanced than ozone production: 5–12 times versus 2–7 times. They observed minimal enhancement of ozone and NO_2 concentrations and slight enhancement of ozone production in boreal biomass burning plumes while the concentration and production of ΣPNs are significantly enhanced, noting that the latter can act as a source and enhance ozone production downwind of the plume. Consistent with these results, Thompson et al. (2011) using the laminar identification (LID) method (Thompson et al., 2007a, 2007b) and ARC-IONS (ARCtic Intensive Ozonesonde Network Study) data showed that the fire contribution could be up to about 5% of tropospheric ozone at the Goose Bay site, far downwind of fire activity in central Canada.

In this study ozonesonde profiles collected in June, July and August of 2006, 2008, 2010 and 2011 from 18 sites across North America north of 40° N latitude are used to determine ozone enhancement empirically. The method developed here is independent of chemical modelling and can be applied to all ozonesonde data collected from regular and campaign sites as long as fire data are available. This method is applicable to evaluating the contribution of biomass burning to the ozone budget as the observations are from a network across northern North America and (unlike typical aircraft observations) are not selected for proximity to fires or fire plumes.

2. Data and methods

2.1. Ozonesonde data

Fig. 1 shows the locations of ozonesonde launch sites across Canada and the US that participated in the IONS (INTEX Ozonesonde Network Study) and BORTAS campaigns (Palmer et al., 2013; Parrington et al., 2012; Tarasick et al., 2010; Thompson et al., 2007a). Table 1 and Table 2 describe the geolocation of these stations (latitude, longitude, and elevation), and the numbers of profiles available from each study. A total of 1110 profiles from sites north of 40° latitude have been used here (Fig. 1 and Table 2). Two types of ECC ozonesondes, the EnSci Corp. 2Z model and the Science Pump 6A, with minor differences in construction and preparation, were used at different sites. The maximum likely variation in tropospheric response resulting from these differences is of the order of 2% (Smit et al., 2007), and for these purposes is a negligible source of error. Measurement precision is ±3–5% and the overall uncertainty in ozone concentration is less than 10% in the troposphere (Smit et al., 2007; Tarasick et al., 2016, 2019b,c).

The ozonesonde sensor response time (e^{-1}) is about 25 s. For a typical balloon with ascent rate of 4 m s^{-1} in the troposphere this implies a vertical resolution of about 100 m. Pressure and temperature data measured by the coupled radiosonde were used to calculate altitude using the hydrostatic relation. Tropopause height is determined using the World Meteorological Organization thermal lapse rate criterion: the lowest height at which the temperature lapse rate falls to 2 °C/km or less, provided that the average lapse rate for 2 km above this height is also not more than 2 °C/km (WMO, 1957). All ozonesonde profiles have been processed to 100 m altitude resolution up to tropopause height or 15 km, whichever is reached first. Ozone partial pressures are averaged for 100 m thick layers from sea level up to the top of the profile. Dividing by the average pressure in each layer, the average ozone mixing ratio is obtained.

2.2. Fire data

MODIS (MODerate Image Spectroradiometer) fire data Collection 5 (Giglio et al., 2003) are used to determine the locations of fire hotspots. Fig. 2 shows the location and intensity of boreal fires between June and August of 2006, 2008, 2010, and 2011. The total area burned was above the long-term average (2.1 million ha) for 2006, 2010, and 2011 (Fig. 3). Among those years, 2006 had the largest number of fires with more than 9800 fires (Fig. 3), while for the others it was below the long-term average of 8000 fires (Canada's National Forestry Database, 2019). Fig. 4 shows examples of ozone peaks in sonde profiles, as well as the corresponding back-trajectories which appear to indicate the influence
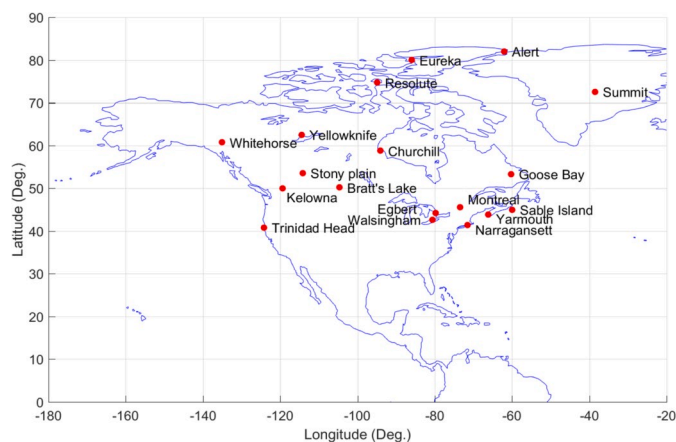

Fig. 1. Location of stations assigned for ARC-IONS and BORTAS campaigns and used for this work.

Table 1

Locations of the sites participating in the IONS-06, ARC-IONS and BORTAS campaigns.

Site Name	ID	Lat	Lon	Alt
Alert	18	82	−62	47
Eureka	315	79.99	−85.94	10
Resolute	24	74.71	−94.97	46
Summit	491	72.57	−38.48	3238
Whitehorse	–	60.7	−135.07	704
Yellowknife	–	62.5	−114.48	210
Churchill	77	58.74	−94.07	30
Trinidad Head	445	40.8	−124.16	20
Kelowna	457	49.92	−119.4	456
Stony Plain	21	53.55	−114.11	766
Bratt's Lake	338	50.2	−104.7	1550
Walsingham	482	42.64	−80.57	182
Egbert	456	44.23	−79.78	251
CSA-Montreal	496	45.51	−73.39	35
Narragansett	487	41.4	−71.5	23
Yarmouth	458	43.87	−66.1	9
Goose Bay	76	53.32	−60.3	44
Sable Island	480	44.95	−59.92	4

of large fire activity.

2.3. Trajectory model calculation

The HYSPLIT (Hybrid Single-Particle Lagrangian Integrated Trajectory) model (Draxler and Hess, 1998) developed by the National Oceanic and Atmospheric Administration Air Resources Laboratory (NOAA ARL), was used to calculate backward trajectories for each ozonesonde profile at 100 m height intervals (50 m, 150 m, etc.). An air parcel is assumed to be released at each 100 m altitude above the location of the ozonesonde station (release time, latitude, and longitude are taken from the ozonesonde launch). The meteorological input for the trajectory model is the global NOAA-NCEP/NCAR (National Centers for Environmental Prediction/National Centre for Atmospheric Research) reanalysis data set (Kalnay et al., 1996). These data provide 4-times-daily meteorological parameters at 17 pressure levels from 1000 to 10 hPa with 2.5 × 2.5° horizontal resolution. This relatively coarse vertical resolution (corresponding to 2 km in the upper troposphere) implies that trajectories are not entirely independent, a point that needs to be kept in mind when estimating statistical significance. Nevertheless, the vertically dense set of trajectories gives some information about sensitivity to initial conditions; the fact that trajectories launched 100 or 200 m apart gave similar results despite their somewhat different paths

allows some confidence that the results found below are robust. Six days (144 h) of backward trajectories were computed for each air parcel.

Several studies have attempted to estimate the accuracy of trajectories using different methods. Stohl (1998) found typical errors of 20% of the trajectory distance, or about 100–200 km/day. More recently, Harris et al. (2005) reported uncertainties of 30–40% of the horizontal trajectory distance, or 600–1000 km after 4 days, while Engström and Magnusson (2009), using an ensemble analysis method, estimated the uncertainty of trajectories to be within 350–400 km after 3 days and about 600 km after 4 days. These are consistent with the Stohl (1998) estimate.

2.4. Example of elevated ozone layers

Fig. 4 illustrates elevated ozone layers detected in ozone profiles collected at a site downwind of near large fire activity (Yarmouth). The MODIS fire hotspots for six days preceding the ozonesonde measurements show large fires in central Canada. Six-day back-trajectories suggest that the layers of high ozone have crossed an area of large fire activity before arriving at the sounding site location. The humidity profile is also depicted. While the layers with high ozone at 6 km trace back over the fires, they are also associated with low humidity, suggesting the possibility of descent from the stratosphere (e.g. Bourqui et al., 2012; Van Haver et al., 1996; Newell et al., 1999; Stohl et al., 2000). Transport from the stratosphere is also a source of high ozone layers in the troposphere. In the next section a method is developed to remove suspected stratospheric layers from the calculation.

2.5. Stratospheric ozone intrusions

Intrusions of ozone-rich air from the stratosphere, stratosphere-troposphere transport (STT), are phenomena that frequently perturb the tropospheric ozone profile (Newell et al., 1999). Observations suggest that tropospheric dry layers associated with high ozone are often STT events (Colette and Ancellet, 2005; Hocking et al., 2007; Newell et al., 1999; Stohl et al., 2000; Thompson et al., 2007a; Van Haver et al., 1996; Vérèmes et al., 2017), and the relative humidity/ozone relationship is frequently used as a simple indicator of probable stratospheric origin (e.g. Bourqui et al., 2012; Cristofanelli et al., 2006; Tarasick et al., 2019a).

To avoid a potential bias in the calculations presented here, suspected stratospheric intrusions were removed from the ozone profiles. The identification of STT was based on the relative humidity-ozone relationship. The suspect layers were determined through the
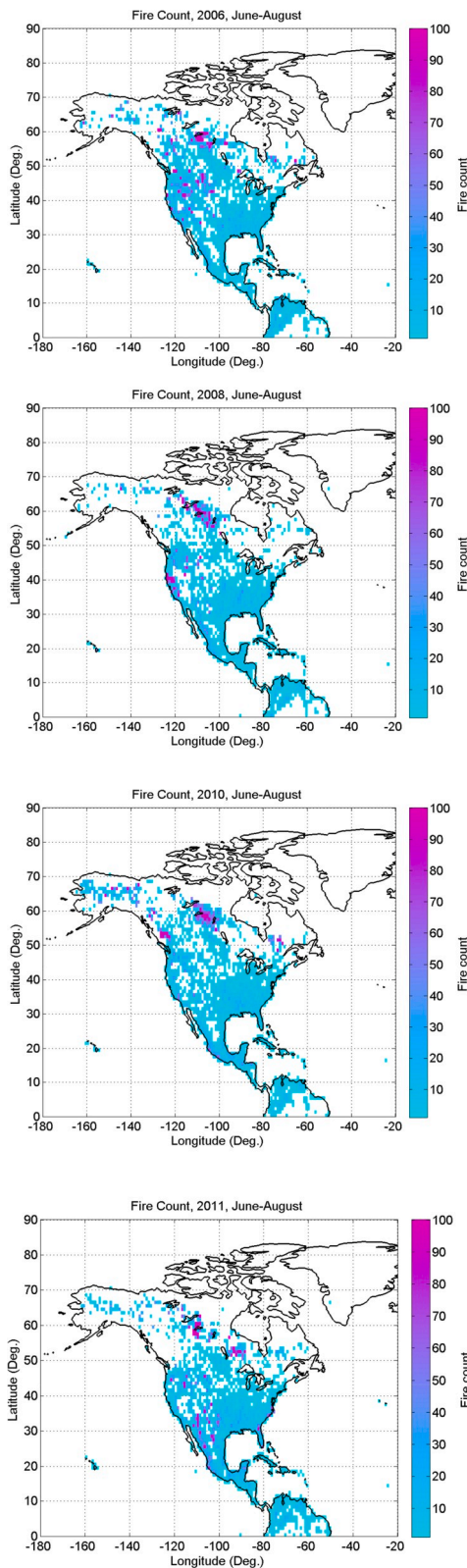
Table 2

Number of profiles, by month and year, measured at different sites.

Site Name	2006			2008			2010			2011			Total
	Jun	Jul	Aug	Jun	Jul	Aug	Jun	Jul	Aug	Jun	Jul	Aug	
Alert	4	3	5	4	4	5	4	2	2	3	3	4	43
Eureka	3	4	5	4	4	5	5	3	3	5	4	5	50
Resolute	3	1	0	3	5	3	4	2	3	2	2	1	29
Summit	5	4	2	15	26	4	3	2	4	5	4	5	79
Whitehorse	0	0	0	4	11	0	0	0	0	0	0	0	15
Yellowknife	0	0	0	7	11	0	0	0	0	0	0	0	18
Churchill	4	4	4	8	8	1	2	4	3	5	1	1	45
Trinidad Head	5	4	30	10	15	4	18	3	4	4	4	4	105
Kelowna	5	2	27	8	13	4	18	2	3	2	3	5	92
Stony Plain	4	1	4	8	14	3	5	4	3	5	4	5	60
Bratt's Lake	4	2	29	6	11	4	4	17	4	4	21	5	111
Walsingham	0	0	22	0	0	0	0	12	0	0	0	0	34
Egbert	3	4	15	1	12	3	4	20	5	5	17	4	93
CSA-Montreal	0	0	0	0	0	0	0	14	0	0	0	0	14
Narragansett	4	4	24	4	3	5	2	2	2	0	0	0	50
Yarmouth	3	3	11	8	14	1	5	20	8	5	20	7	105
Goose Bay	3	2	5	4	11	0	4	18	8	4	22	7	88
Sable Island	0	0	28	4	11	0	0	16	0	0	19	1	79
Total	50	38	211	98	173	42	78	141	52	49	124	54	1110

Fig. 2. Modis fire hot spots during Jun.–Aug. 2006, 2008, 2010, and 2011.

following steps (all steps were applied to the entire ozone profile):

1. A mean, or baseline, profile was obtained by boxcar-smoothing the high-resolution profile to remove variations of vertical half-width less than 2.5 km. The difference between the high-resolution
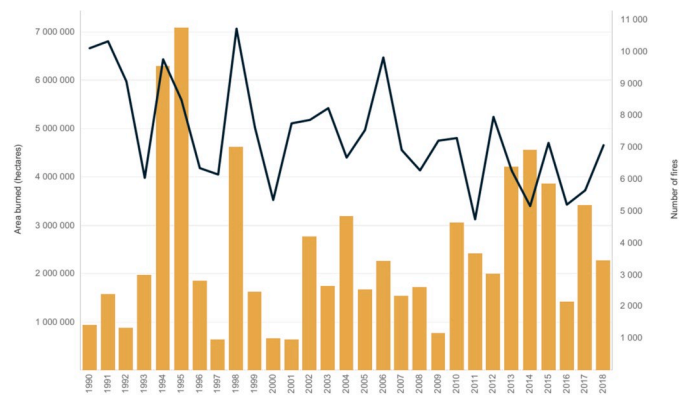

Fig. 3. Area burned (brown bars) and number of fires (black line) in Canada between 1990 and 2018; Retrieved from National Forestry Database (http://nfdp.ccfm.org/en/data/fires.php; last access 29-09-2019). (For interpretation of the references to color in this figure legend, the reader is referred to the Web version of this article.)
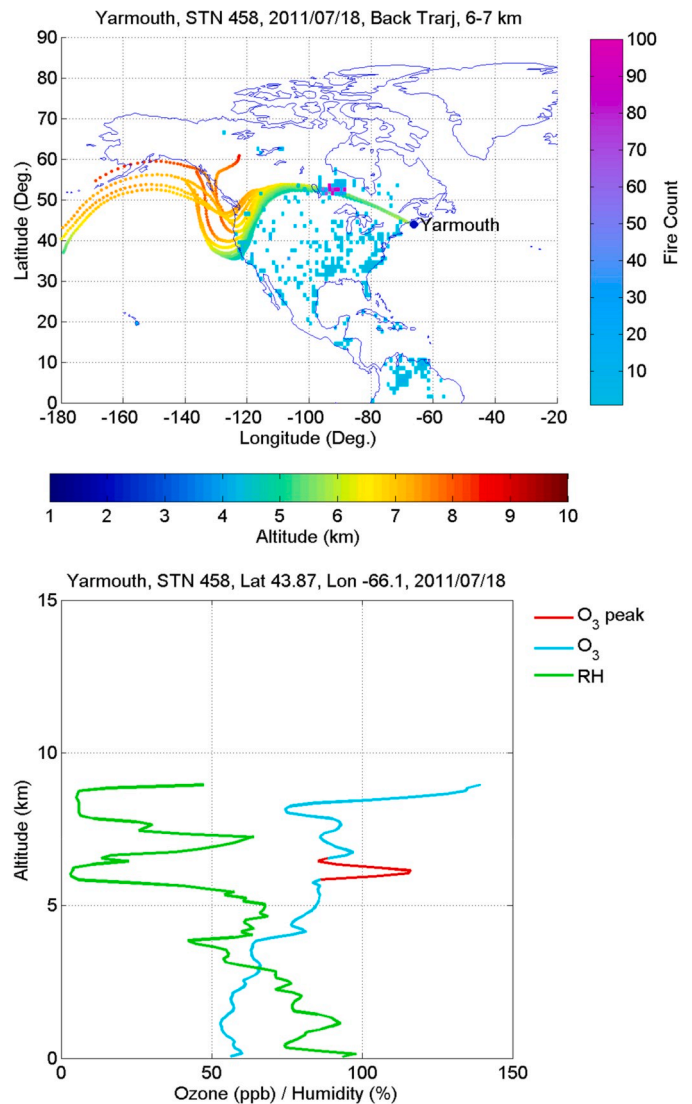

Fig. 4. (Lower panel) Ozone and humidity profiles for July 18, 2011 at Yarmouth. (Upper panel) Back-trajectories indicate that the ozone anomalies could be produced by fires. Note that in both profiles high ozone layers are associated with low humidity.

profile and the mean profile, divided by the mean profile, was calculated and defined as the normalized perturbation profile.

2. The same method was used to determine a normalized perturbation profile of relative humidity (RH). Boxcar averaging was used to filter out variations of vertical half-width less than 5 km from the RH profile, to find mean RH profile.

3. Ozone laminae with average amplitudes greater than 10% of the mean ozone mixing ratio were considered as being of stratospheric origin and removed from the profile if associated with negative RH laminae with average amplitudes greater than 20% of the mean relative humidity.

These thresholds are similar to those used by Newell et al. (1999). The number of STT layers identified in this way is not greatly sensitive to the choice of these parameters (Tarasick et al., 2019a).

Fig. 5 shows an ozone profile with a large anomaly between 5 and 6 km. Back trajectories (shown in the top panel) and the tropopause height map (shown in the second panel) indicate that for much of their paths over northern Canada these air parcels were close to the tropopause, suggesting a possible stratospheric origin for these parcels. Tropopause height data were provided by the NOAA Physical Sciences Division (http://www.esrl.noaa.gov/psd) from the same NCEP/NCAR reanalysis database used as input to the HYSPLIT model (Kalnay et al., 1996). The WMO (1957) thermal lapse rate criterion was used to compute tropopause heights, with the additional criterion that tropopauses at pressure levels smaller than 85 hPa or larger than 450 hPa were not allowed by the NOAA calculations.

The third panel illustrates the identification of this layer as a suspected stratospheric intrusion by the algorithm described above. The portion of the profile shown in red is excluded from further calculations. There are a number of observations that stratospheric intrusions are sometimes associated with, and apparently can affect fires (Charney et al., 2003; Langford et al., 2015; Zimet et al., 2007). Since it is not entirely clear that these two potential sources of tropospheric ozone can be separated, the DBT calculations were performed with STT layers removed, as described above, and also without any STT removal. On average about 30% of parcels were identified as originating from the stratosphere using this method, with more in the upper troposphere than the lower troposphere. However, suspected STT layers appeared in the fire-affected profiles with about the same frequency and same amount of ozone as in the background (fire-unaffected) profiles, so no significant difference in the overall results was found, and the remainder of this paper discusses only the results for which suspected STT layers, in all profiles, were excluded from further calculations.

2.6. Differential back trajectory (DBT) method

The DBT method uses back-trajectories calculated at 100 m intervals from the surface to the tropopause, for each sounding, up to 144 h long (six days). A parcel is defined as "fire-affected" if the back-trajectory corresponding to a parcel passes through a 1×1-degree grid box containing one or more MODIS fire counts. The remaining parcels are classified as background or "fire-unaffected". For this study, only parcels that are affected by fires in North America were considered as "fire-affected". Parcels affected by fires outside this zone (e.g. Asia, South America, etc.) were removed from the analysis. At each 100 m level, for each sonde site, the average difference in ozone concentration associated with "fire-affected" parcels in each year and "fire-unaffected" parcels from all four years (2006, 2008, 2010, and 2011) is calculated. To calculate the average fire contribution to ozone, the computed average ozone difference is multiplied by the ratio of the number of "fire-affected" parcels to the total number of parcels (sum of "fire-affected" and "fire-unaffected") for that specific year. Suspected stratospheric intrusions, STT (identified as layers of high ozone coincident with low RH), are first removed from all profiles as described above, to avoid skewing the averages. The ensembles of average "fire-

affected" and "fire-unaffected" parcels for Yarmouth station for the 2010 season are depicted in Fig. 6.

The DBT method offers a statistical estimate of the amount of additional ozone generated by fires. It neglects any contribution from fires more than 144 h previous to the sounding. This is likely a small error, since back-trajectories from any of the sonde sites will generally cross the continent in less than 6 days. A more important source of error is the mis-assignment of air parcels due to trajectory errors: any systematic difference in average ozone concentration between "fire-affected" and "fire-unaffected" air parcels will be diluted by such mis-assignment. Since trajectory errors over several days can be quite large (Downey et al., 1990; Engström and Magnusson, 2009; Harris et al., 2005; Stohl, 1998), this probably causes the DBT method to produce a serious underestimate of the amount of ozone generated by fires; that is, the DBT estimates of fire ozone are conservative.

3. Results and discussion

3.1. Ozone enhancements

The intensity and location of fires is quite variable. As shown in Fig. 2, large fire activity in 2006 was concentrated in Central Canada, the Western U.S. and Southern U.S. The average total tropospheric ozone calculated from fire-unaffected parcels is depicted in Fig. 7, in Dobson Units (DU), and the average enhancement in total tropospheric ozone column (TTOC) due to fire activity over four years (2006, 2008, 2010 and 2011) is shown for 18 sites in Fig. 8. The analysis shows that none of the high latitude sites has been affected significantly. This may be due in part to the fact that fires in Asia and Europe are not considered (Section 2.6). Overall, Narragansett and Yarmouth had the largest ozone enhancements. Kelowna and Stony Plain were not affected significantly although they were occasionally close to large fire activity.

Average ozone enhancements calculated by the DBT method for each site in 2006, 2008, 2010, and 2011 (June–August) are shown in Fig. 9 in (DU), and compiled in percentage in Table 3. The fire contribution in 0–5 km column ozone was statistically significant at 8 sites out of 14 in 2006, ranging between 0.4 ± 0.2 and 2.0 ± 1.2 DU (1.2 ± 0.6 and $4.3 \pm 0.4\%$) with a minimum in Stony Plain and a maximum at Bratt's Lake. In terms of TTOC, 4 sites were significantly affected. The fire ozone contribution to TTOCs at Trinidad Head and Bratt's Lake, which were close to large fires (Fig. 2), was 1.3 ± 0.3 DU ($4.1 \pm 0.6\%$) and 0.7 ± 0.5 DU ($2.0 \pm 1.2\%$), respectively. The ozone enhancements for Yarmouth, and Sable Island (downwind sites) were 2.2 ± 0.5 DU ($4.7 \pm 1.1\%$) and 1.3 ± 0.5 DU ($2.8 \pm 1.0\%$), respectively.

Two large fire events occurred during the summer of 2008 (Fig. 2). One was caused by large fires in Saskatchewan in central Canada and the other was in the western and midwestern U.S. Ozone profiles from 16 sites were used to calculate average fire ozone amounts during June to August 2008. The DBT method finds that fire ozone significantly contributed to the TTOC of 6 sites during 2008.

Trinidad Head was the closest to the U.S. fires in 2008. Fire ozone accounted for 1.5 ± 0.4 DU ($4.2 \pm 0.8\%$) of TTOC at this station. Bratt's Lake was also nearby large fires in Canada. The ozone enhancement for Bratt's Lake was 0.8 ± 0.5 DU ($2.2 \pm 1.3\%$). Narragansett, Yarmouth, Goose Bay, and Sable Island were also significantly affected by fires. Fire ozone contribution in the TTOC was computed, respectively, as 2.0 ± 0.8 DU ($4.4 \pm 1.8\%$), 2.0 ± 0.5 DU ($4.3 \pm 1.0\%$), 1.9 ± 0.4 DU ($5.2 \pm 1.0\%$) and 4.0 ± 0.6 DU ($8.3 \pm 1.3\%$) for these sites. Large Canadian fires in 2008 took place near to five Canadian sites: Yellowknife, Whitehorse, Churchill, Kelowna and Stony Plain. Although these sites show some enhancement in the 0–5 km (above ground) ozone columns, TTOCs were not significantly enhanced.

2010 was an exceptional year in terms of total area burned by Canadian boreal fires (Fig. 3). Large fire events were recorded in North Central and Western Canada (Fig. 2). Ozonesonde data are available at 13 regular sites, plus Walsingham, Montreal and Narragansett. Of the

Sable Island, STN 480, 2010/07/26, Back Traj, 5-6 km

Tropopause Height, 2010/07/23

Sable Island, STN 480, Lat 43.93, Lon -60, 2010/07/26
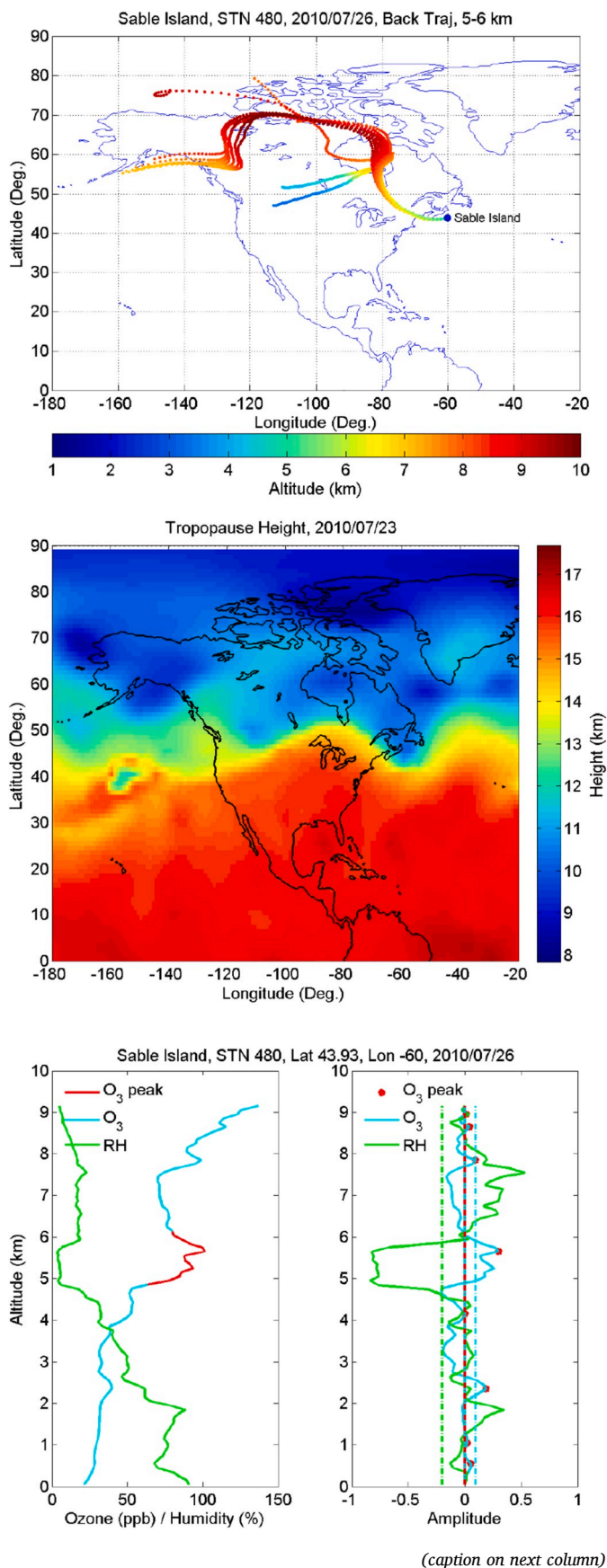
(caption on next column)

Fig. 5. (Top) back-trajectories for the layers between 5 and 6 km indicate the possibility of stratospheric intrusions. (middle) Tropopause height retrieved from NCEP/NCAR reanalysis data (Kalnay et al., 1996). (bottom) Identification of a suspected stratospheric intrusion by algorithm described in text. Ozone and relative humidity profiles of July 26, 2010 at Sable Island. The portion of the profile shown in red in the left-hand plot is excluded from further calculations. Other ozone peaks, indicated by red dots in the right-hand plot, are either not large enough, or not associated with large negative changes in relative humidity, and so are not excluded. (For interpretation of the references to color in this figure legend, the reader is referred to the Web version of this article.)

sites close to the fires, Bratt's Lake was significantly affected with ozone enhancement of 1.8 ± 0.5 DU ($4.8 \pm 1.3\%$). Fire ozone accounted for 1.4 ± 0.4 DU ($3.1 \pm 0.9\%$), 3.6 ± 0.9 DU ($8.1 \pm 2.1\%$), 2.1 ± 0.4 DU ($4.4 \pm 1.0\%$), 0.6 ± 0.4 DU ($1.6 \pm 1.0\%$) and 0.8 ± 0.4 DU ($1.6 \pm 0.9\%$) of the TTOC at the downwind sites: Egbert, Narragansett, Yarmouth, Goose Bay, and Sable Island, respectively.

The number of fires in 2011 was about 4200 which is about half of the long-term average of 8000 fires in Canada (Fig. 3). The ozone profiles collected by 11 Canadian sites, plus Summit and Trinidad Head were used to calculate the influence of fires on tropospheric ozone at downwind sites. Only two sites were significantly affected by fires, Egbert where 2.0 ± 0.4 DU ($4.4 \pm 0.9\%$) ozone enhancement was detected, and Yarmouth with 1.8 ± 0.4 DU ($3.8 \pm 0.8\%$) fire ozone contribution in the TTOC. Ozone in the 0–5 km column was also enhanced at the Churchill and Stony Plain sites. Surprisingly, the analysis shows that Sable Island was negatively affected by fires in 2011. Although apparent ozone destruction in boreal fire plumes has been reported previously (Real et al., 2007; Verma et al., 2009), this is likely an indication of the magnitude of possible error in this statistical method. Generally, the DBT method finds that downwind sites were more affected by fires than the sites nearer to the large fires indicating the transport of ozone and/or its precursors from fire locations to downwind locations.

3.2. Validation and sensitivity tests of the DBT method

Several variations or refinements of the DBT method are possible, and these can be used to test the sensitivity of the method to variations of the parameters used to classify trajectories.

3.2.1. Fire plume injection height

The foregoing analysis treats all trajectories that pass over a grid box containing one or more MODIS fire counts as "fire-affected". This is clearly a weak assumption, as fire plume height and the altitude range influenced are highly variable, depending on fire size and intensity and also on atmospheric conditions (Freitas et al., 2007; Kahn et al., 2008; Labonne, 2007). Different approaches have been used to develop algorithms and models to determine the appropriate injection heights for biomass burning emissions (Freitas et al., 2007; Kaiser et al., 2012; Paugam et al., 2016; Sofiev et al., 2012), but no general formula has emerged. Studies show that fire plumes are likely able to reach 10 km altitude or even into the lower stratosphere depending on fire radiative power (FRP) and fire size (Freitas et al., 2007). For this modified calculation, it is assumed that larger fires provide higher injection heights. The size of fires is determined by counting the fire hotspots in each $1 \times 1°$ grid box over 24 h. Table 4 shows the assumed smoke plume height for a given MODIS fire count. In this calculation, both altitude and fire count are considered to identify the fire-affected parcels. For example, if the back-trajectory corresponding to a parcel passes through a 1×1-degree grid box containing 1–10 fire counts that parcel only is identified as fire-affected if its altitude is 0–2 km; otherwise it is excluded from the analysis. As before, the remaining parcels are classified as background or fire-unaffected. After applying assumed fire plume injection heights into the DBT method, the contribution of fire ozone to TTOC is calculated. Fig. S1 shows the results for Yarmouth
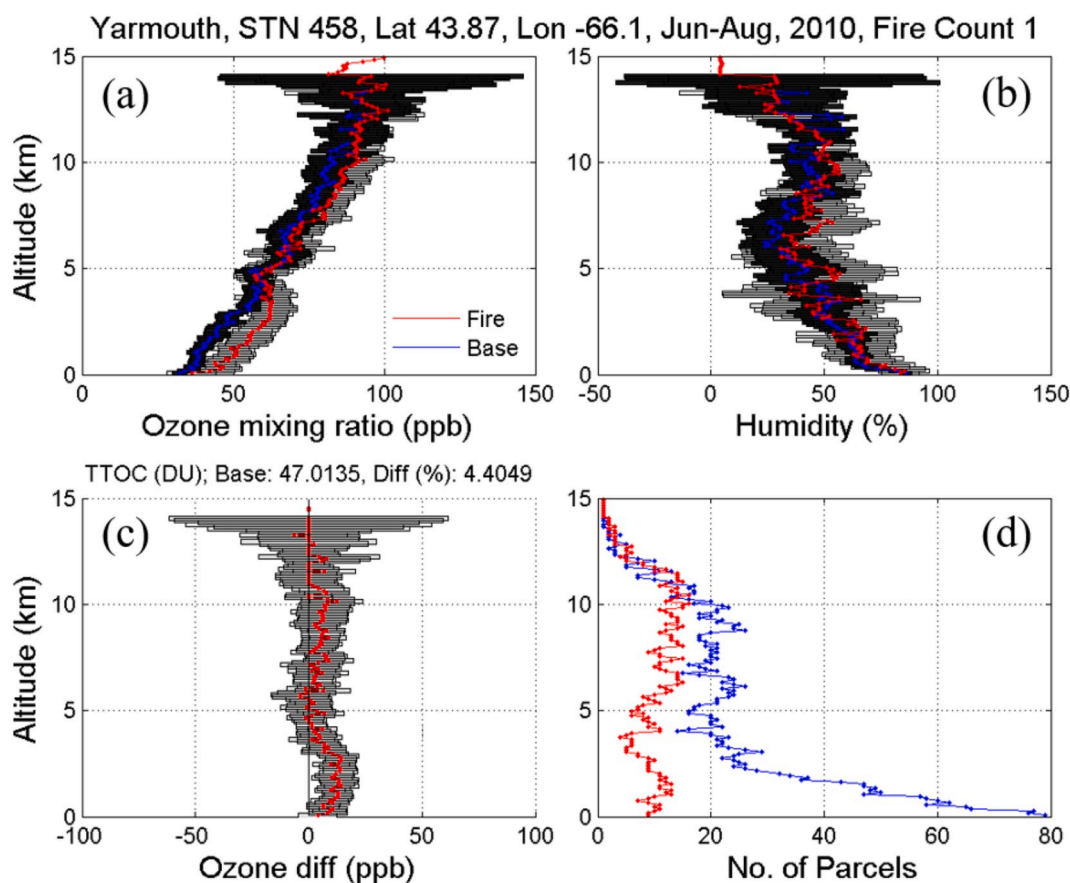
Fig. 6. Example of results from the Differential back trajectory (DBT) method, for Yarmouth, NS. (a, b): average ozone and humidity for fire-affected (Fire, red) and non-affected (Base, blue) parcels. The error bars equal 2 standard errors (SE). (c): average difference between fire-affected and non-affected parcels. Total Tropospheric Ozone Column (TTOC) calculated from non-affected parcels (Base) is also depicted in DU along with the percentage difference (Diff). (d): number of fire affected (red) parcels during summer 2010 and number of non-affected (blue) parcels over four years (2006, 2008, 2010, and 2011). (For interpretation of the references to color in this figure legend, the reader is referred to the Web version of this article.)
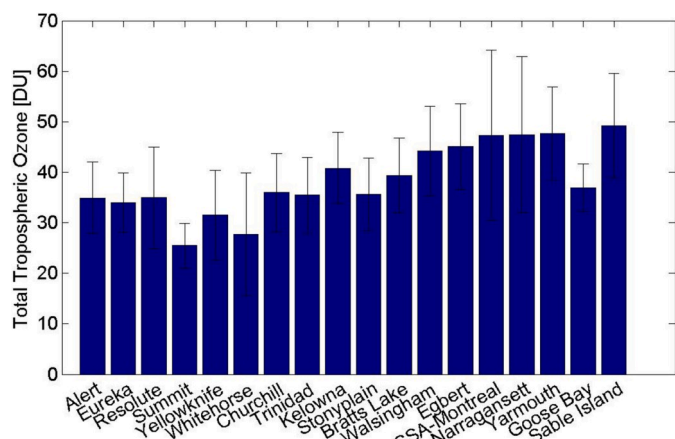
Fig. 7. Average total tropospheric ozone over 2006, 2008, 2010 and 2011 expressed in DU calculated from fire-unaffected parcels. Error bars indicate 2 SE. Arctic and northern latitude sites (first 7 sites starting by Alert) are ordered by latitude. The rest (starting by Trinidad) are ordered by longitude from West (nearby sites) to East (downwind sites).

Fig. 8. Average enhancement in total tropospheric ozone column due to fire activity at different sites over 2006, 2008, 2010, and 2011. Error bars indicate 2 SE. Sites ordered as in Fig. 7.

station for 2010 season the same as Fig. 6 but taking into account the fire plume heights inferred from Table 4.

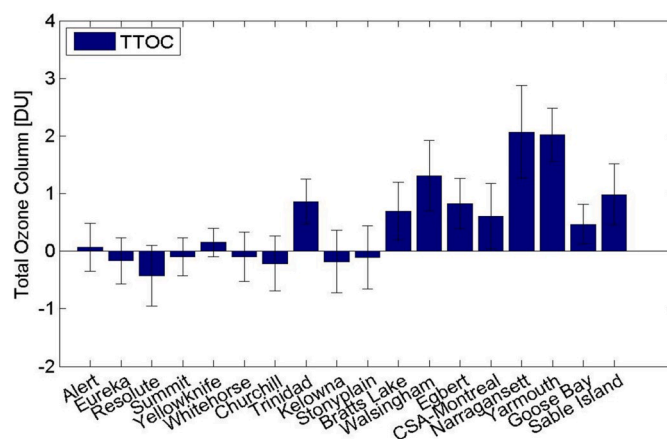The average ozone enhancements in TTOC over four years are displayed in Fig. 10. The imposition of an injection height criterion reduces the number of fire-affected parcels by about 2/3, so the error bars are much larger, but the results are more uniformly positive compared to those in Fig. 8. The calculated contributions of fire ozone to TTOC are still positive and significant for most of the sites. On average, the lowest significant enhancement in TTOC was at Sable Island with 0.5 ± 0.5 DU (1.1%) and the largest occurred over Yarmouth with 1.2 ± 0.4 DU (2.6%) followed by Narragansett and Montreal with 1.0 ± 0.8 DU. Seven
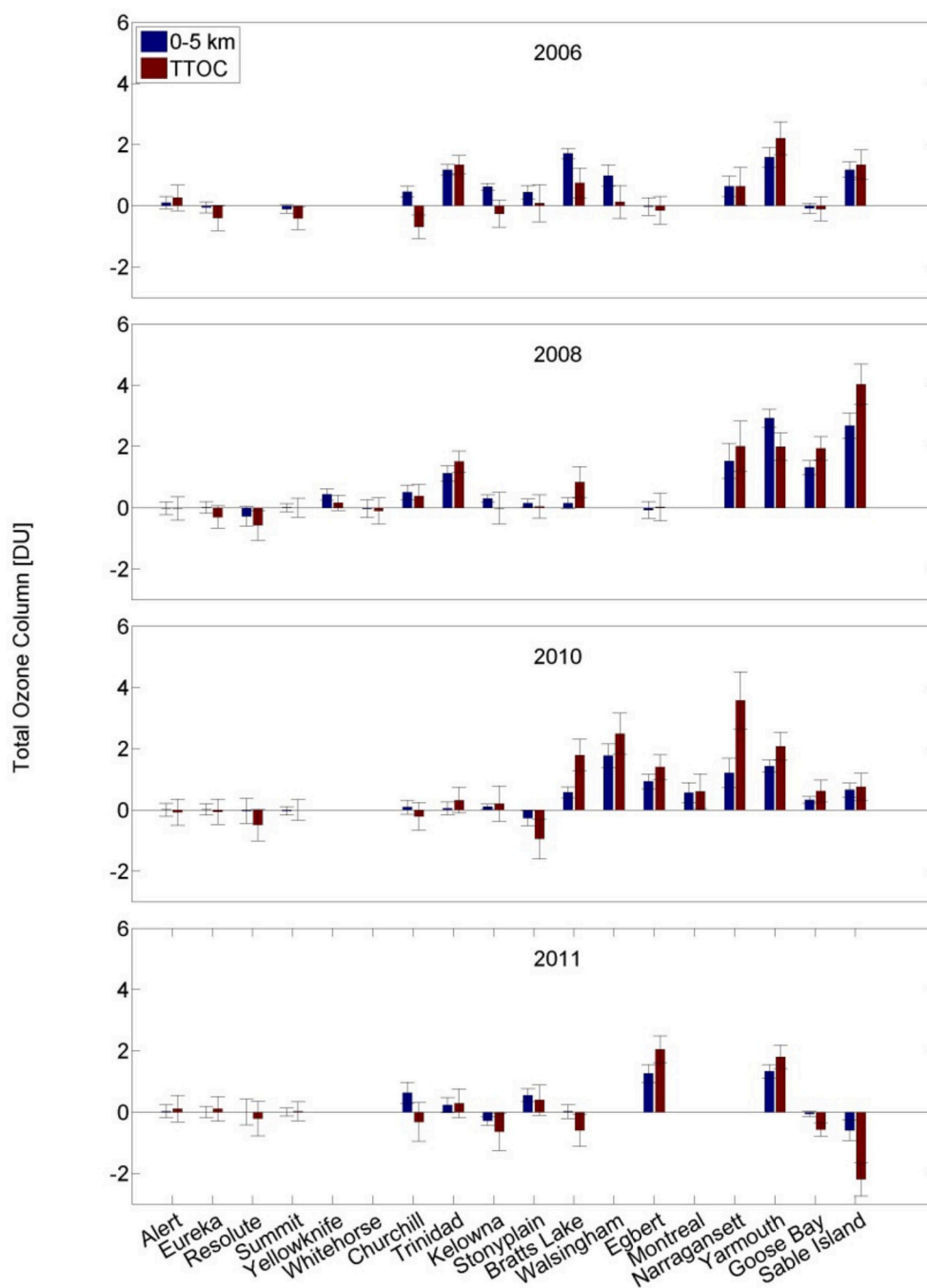
Fig. 9. Average enhancement in 0–5 km and total tropospheric column ozone (TTOC) at different stations during the 2006, 2008, 2010, and 2011 summer, expressed in DU. Error bars indicate 2 SE. Sites ordered as in Fig. 7.

sites – Trinidad Head, Walsingham, Egbert, Montreal, Narragansett, Yarmouth, and Sable Island – were significantly affected by fires. The enhancements over the sites nearer the largest fire activity, such as Bratt's Lake, Stony Plain, and Kelowna are positive but not statistically significant at the 2σ level. As in the previous analysis, none of the Arctic sites was affected significantly, but here the effects are more uniformly positive. Fig. 11 shows the ozone enhancements in TTOC and 0–5 km over each site in 2006, 2008, 2010, and 2011. Comparing to Fig. 9, the imposition of an assumed smoke plume height influenced Sable Island the most by reducing the fire ozone contribution in 2008 from 4.0 ± 0.6 DU (8.3%) to 1.5 ± 0.5 DU (3.1%), but also reducing to non-significance the negative fire contribution in 2011. The injection height criterion lowers the positive ozone enhancements by 0.2–2.6 DU over other sites,

while mostly removing the negative values in Fig. 9.

3.2.2. Possible regional bias in the origin of air parcels

The initial O_3 concentration of air masses could be a source of error in the DBT method. For instance, if many of the fire-affected parcels come from areas with higher background ozone levels (e.g. the southern US), while more fire-unaffected parcels originate from areas with low levels of background ozone, the results could show a difference that is not necessarily related to fire activity. To investigate the contribution of different areas to fire ozone enhancements six geographical regions were defined to tag the parcels based on their origins: Arctic (ARC); Northwest America (NW); Central Canada (CCA); East Canada (ECA); East US (EUS); Southeast US (SEUS); West US (WUS); Southwest America (SW)

Table 3
Ozone enhancement at 0–5 km and total tropospheric ozone column (TTOC) in % at individual site. Uncertainties are 2 standard error.

STN/Year	2006		2008		2010		2011	
	0–5 km	TTOC	0–5 km	TTOC	0–5 km	TTOC	0–5 km	TTOC
Alert	0.3 ± 0.6	0.7 ± 1.2	−0.1 ± 0.6	−0.1 ± 1.1	0.0 ± 0.6	−0.2 ± 1.2	0.1 ± 0.6	0.3 ± 1.2
Eureka	−0.2 ± 0.5	−1.2 ± 1.2	0.0 ± 0.6	−0.9 ± 1.1	0.0 ± 0.5	−0.2 ± 1.2	0.0 ± 0.5	0.3 ± 1.2
Resolute	–	–	−0.8 ± 0.9	−1.6 ± 1.4	−0.1 ± 1.2	−1.4 ± 1.5	0.0 ± 1.2	−0.6 ± 1.6
Summit	−0.4 ± 0.5	−1.6 ± 1.5	0.0 ± 0.5	0.0 ± 1.2	−0.1 ± 0.6	0.0 ± 1.3	0.0 ± 0.5	0.1 ± 1.2
Yellowknife	–	–	1.4 ± 0.6	0.5 ± 0.8	–	–	–	–
Whitehorse	–	–	−0.1 ± 1.0	−0.3 ± 1.5	–	–	–	–
Churchill	1.3 ± 0.5	−1.9 ± 1.1	1.4 ± 0.6	1.1 ± 1.1	0.2 ± 0.6	−0.6 ± 1.3	1.7 ± 1.0	−0.9 ± 1.7
Trinidad Head	3.3 ± 0.5	4.1 ± 0.6	3.2 ± 0.7	4.2 ± 0.8	0.1 ± 0.6	0.9 ± 1.0	0.6 ± 0.7	0.8 ± 1.1
Kelowna	1.5 ± 0.3	−0.6 ± 1.1	0.7 ± 0.3	0.0 ± 1.3	0.2 ± 0.2	0.5 ± 1.4	−0.7 ± 0.4	−1.6 ± 1.5
Stony Plain	1.2 ± 0.6	0.2 ± 1.7	0.4 ± 0.4	0.1 ± 1.0	−0.7 ± 0.7	−2.7 ± 1.8	1.5 ± 0.6	1.1 ± 1.4
Bratt's Lake	4.3 ± 0.4	2.0 ± 1.2	0.4 ± 0.5	2.2 ± 1.3	1.5 ± 0.4	4.8 ± 1.3	0.0 ± 0.6	−1.6 ± 1.0
Walsingham	2.2 ± 0.8	0.3 ± 1.2	–	–	3.9 ± 0.8	1.1 ± 2.8	–	–
Egbert	−0.1 ± 0.6	−0.3 ± 1.0	−0.2 ± 0.6	0.0 ± 1.0	2.0 ± 0.5	3.1 ± 0.9	2.7 ± 0.6	4.4 ± 0.9
CSA-Montreal	–	–	–	–	1.2 ± 0.7	1.3 ± 1.2	–	–
Narragansett	1.3 ± 0.7	1.3 ± 1.3	3.4 ± 1.3	4.4 ± 1.8	2.7 ± 1.1	8.1 ± 2.1	–	–
Yarmouth	3.3 ± 0.7	4.7 ± 1.1	6.2 ± 0.6	4.3 ± 1.0	3.0 ± 0.4	4.4 ± 1.0	2.7 ± 0.5	3.8 ± 0.8
Goose Bay	−0.2 ± 0.5	−0.3 ± 1.1	3.6 ± 0.6	5.2 ± 1.0	0.9 ± 0.3	1.6 ± 1.0	−0.2 ± 0.2	−1.5 ± 0.6
Sable Island	2.4 ± 0.5	2.8 ± 1.0	5.3 ± 0.8	8.3 ± 1.3	1.3 ± 0.5	1.6 ± 0.9	−1.2 ± 0.7	−4.7 ± 1.2

Table 4
MODIS fire count and corresponding smoke plume height.

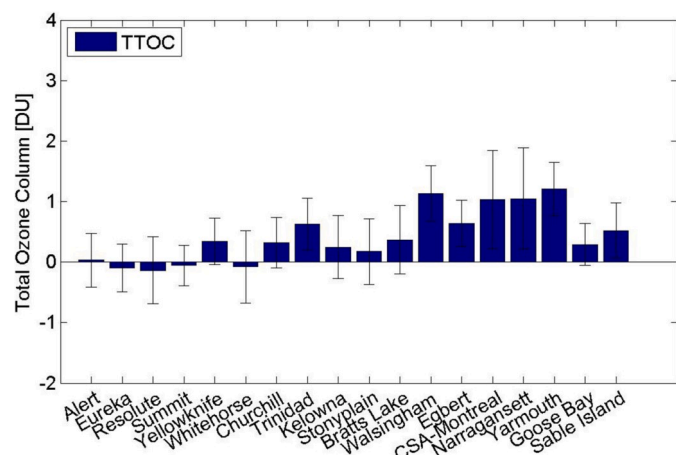| Fire Count	Expected Plume Height
1–10	0–2 km
11–50	2–5 km
51–90	5–7 km
91–120	7–9 km
120<	9 km<

Fig. 10. Average enhancement in total tropospheric ozone column at different sites over 2006, 2008, 2010, and 2011 taking into account the fire plume injection height inferred from Table 4. Error bars indicate 2 SE.

(Fig. S2). The regions were selected based on similarities in ozone climatology and also the record of forest fires. Fig. S3 shows the average total tropospheric column ozone for summer time 2000 to 2009 retrieved from the TOST (Trajectory-mapped Ozonesonde dataset for the Stratosphere and Troposphere) dataset (G. Liu et al., 2013; J. Liu et al., 2013). Regional averages are also shown in the lower left of the figure. As can be seen, there are higher ozone levels over the southern US and Mexico compared to other areas of North America. This is a potential source of error: if a relatively larger number of fire-affected parcels originate in these areas while more background parcels come from lower-ozone areas, a misleading positive signal may be seen at some sites.

Fig. S4 shows the origin of fire-affected parcels for Yarmouth in 2011. The top of the panel illustrates the number of the fire-affected parcels for each year. The number of unaffected parcels is also shown in the last column of the top panel (baseline). The rest of the six pie chart rows show the percentage contribution of each region in total number of parcels for six 24-h periods prior to the ozonesonde lunch time (From 24 h at the top to 144 h at the bottom before the launch time). In the first 24 h, as is expected, the majority of the parcels are in the region of the site location (EUS) and nearby area (ECA). From the second time interval, the contribution of the Central Canada pixels (denoted by an orange color) starts to show an increase for the both fire-affected and unaffected parcels. Evidently, nearly half of the fire-affected and unaffected parcels originated from Central and Eastern Canada 96 h (4 days) before the measurements.

As a sensitivity test, only the parcels originating from Central Canada were considered to calculate the ozone enhancements at downwind sites. Fig. S5 shows the contribution of each region in the number of fire-affected and unaffected parcels after setting this criterion. It can be seen that only parcels that have been in the CCA region (orange color) 72 h before the launch time are used for calculations. Although this criterion excludes about half of the parcels, the results still show significant positive signals for downwind sites and also for the sites closer to large fire activity. Fig. S6 depicts the ozone enhancements in TTOC and the 0–5 km column at different sites in 2006, 2008, 2010, and 2011, considering only air parcels from the CCA region.

In an additional sensitivity test, all trajectories that pass 40°N latitude were removed from the calculations to eliminate the influence of high ozone amounts from the southern US and Mexico. This condition also reduced the number of parcels but minimally affected the outcomes.

A third sensitivity test was conducted using the HYSPLIT clustering tool (See Text S1). Like the previous tests, this showed some variation due the removal of a large portion of the air parcels, and the consequent increase in statistical uncertainty with the smaller sample size. However, the overall results (Fig. 12) are again similar to those in Section 3.1.

In summary, while the possibility of bias in the initial ozone concentration of air masses is a concern for the DBT method, it has no measureable effect on the results we present here. This is because most trajectories over the area of study originate in Canada, with similar background ozone concentrations, and the subset that originate in areas with higher background ozone levels are apparently not over-represented in the fire-affected category.

4. Summary and conclusions

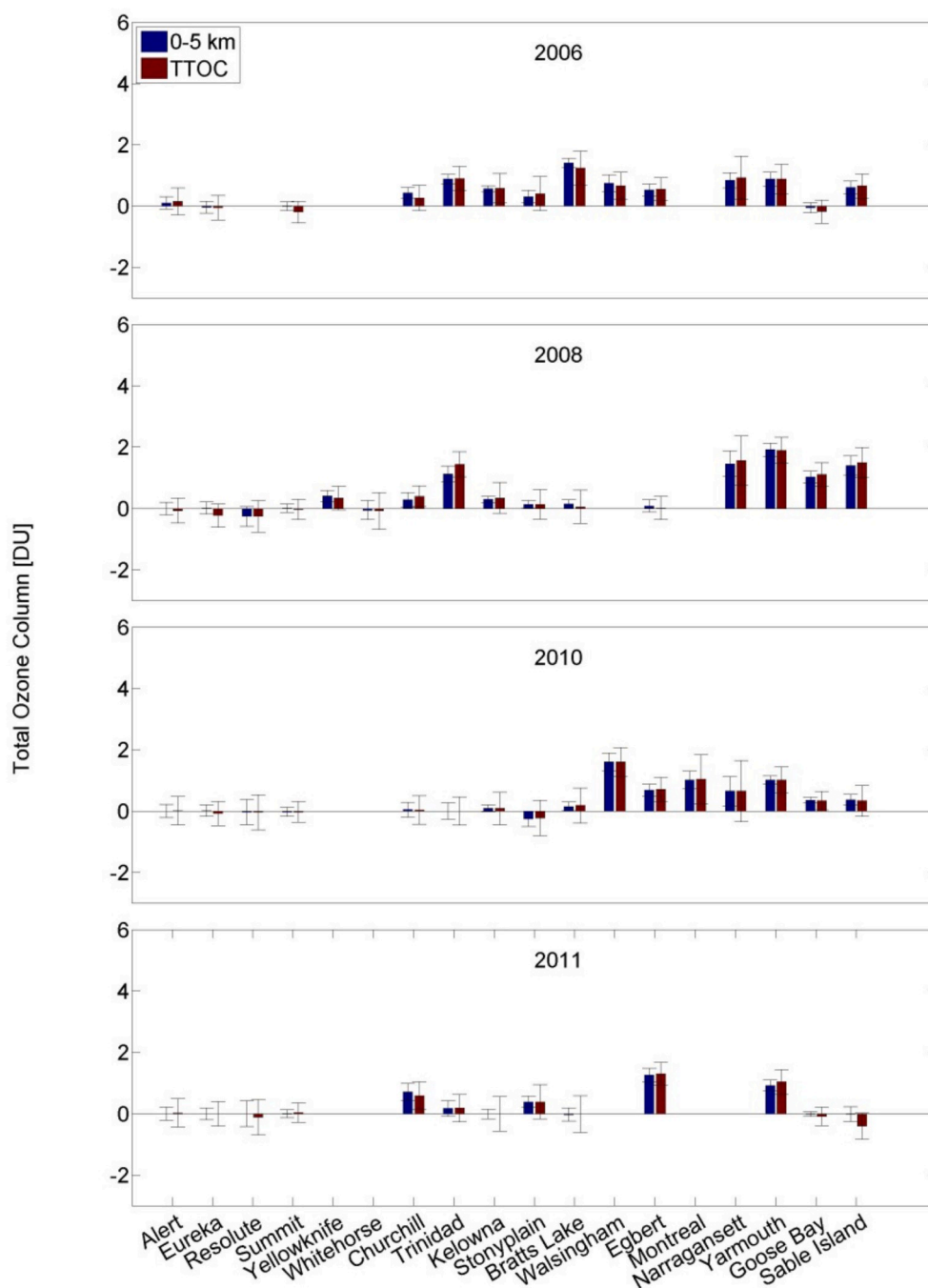Using more than 1100 ozone profiles collected at 18 ozone sounding

Fig. 11. As Fig. 9 but taking into account the fire plume heights inferred from Table 4. Error bars indicate 2 SE.

sites located across Canada and the U.S., in regular sampling and through a number of campaigns in June to August 2006, 2008, 2010 and 2011, this study examines the fire-generated ozone budget in total tropospheric ozone column using HYSPLIT back trajectories. The DBT method is suitable for evaluating the contribution of fire ozone to the tropospheric ozone budget as it uses a network of observing sites at fixed locations across northern North America and so the data (unlike typical aircraft observations) are not selectively sampled for proximity to fires or fire plumes. No significant influence on average ozone levels by North American fires was found for stations located at Arctic latitudes. This may be in large part because we considered only fire sources in North America (Section 2.6). Sources in Eurasia are likely to have an important impact on Arctic sites and should be considered in a more comprehensive study. Sites nearer to the larger fires show less fire ozone, in general,

than sites further away (and downwind). The ozone enhancement for stations near large fires, such as Trinidad Head, Bratt's Lake, Kelowna and Stony Plain was up to 4.8% of the TTOC, while fire ozone accounted for up 8.3% of TTOC at downwind sites such as Sable Island, Yarmouth, Narragansett and Walsingham. Our results are therefore consistent with analyses that report an increase in ozone production with the age of the plume (e.g. Baylon et al., 2015; Busilacchio et al., 2016; Jaffe and Wigder, 2012; Parrington et al., 2013; Real et al., 2007; Teakles et al., 2016; Val Martin et al., 2006; Wigder et al., 2013; Wotawa and Trainer, 2000). These report peak enhancements from 4 to 44 ppbv, with a typical range of 10–20 ppbv, in a variety of plumes aged 5–10 days (with some as old as 15 days). A few studies estimate average enhancements, of up to 13 ppb over the month of August at a mountaintop site (Mac-Donald et al., 2011), and 7–9% of TTOC (~3 DU) in July 2004 (Pfister
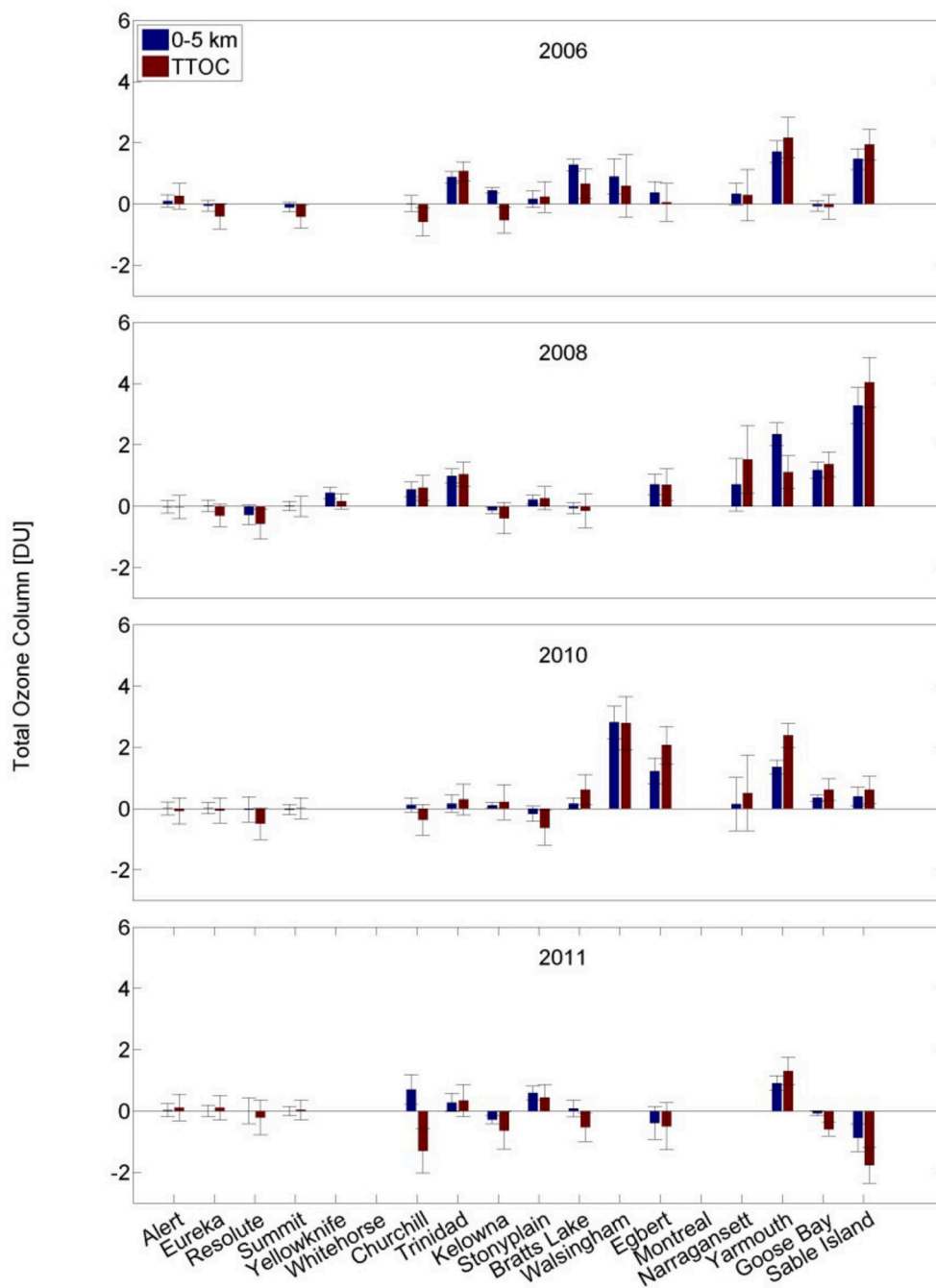
Fig. 12. As Fig. 11 (i.e. fire plume heights have been considered) after removing the profile clusters originating from the southern US.

et al., 2006). The latter studies are easily compared with our results (e.g. Fig. 6c; Fig. 9). We find that over the four-year average, nine sites – Trinidad Head, Bratt's Lake, Walsingham, Egbert, Montreal, Narragansett, Yarmouth, Goose Bay and Sable Island – were significantly influenced by fire ozone. However, we note that the DBT method likely produces an underestimate of ozone production by fires, due to trajectory errors.

Several additional calculations were made to examine the sensitivity of the results to potential biases in input parameters. These included assuming a fire plume height based on fire intensity, and examining differences in background ozone owing to possible biases in the geographic origin of trajectories. The latter calculations included (1) eliminating trajectories that cross certain latitudes (e.g. 40°N or 50°N), (2) a HYSPLIT cluster analysis that eliminated clusters of trajectories that originate in the higher ozone regions of the US, and (3) considering

only parcels that originate in central Canada, a defined region of relatively uniform background ozone. These sensitivity tests indicate that our results are robust with respect to these input criteria, producing similar results, within statistical uncertainty, in each case. However, the criteria chosen for these tests significantly reduced the number of trajectories available for analysis, increasing the statistical uncertainty. We therefore consider the results of the unrestricted DBT method, in Section 3.1, to be the most reliable.

While the uncertainties related to trajectory errors affect the determination of absolute amounts of fire-generated ozone, producing, as we have noted, a likely underestimate of ozone production by fires, this will be much less of a problem for determining relative amounts, and trends with time. The DBT method could be extended to the entire Canadian fire and ozone profile record using more than 50 years of ozonesonde and fire data collected from sites across Canada to better quantify the

impact of wildfires on tropospheric ozone, including a half-century of changes with time.

Data availability

Ozonesonde data including the IONS and BORTAS campaign data are all available from World Ozone and Ultraviolet Radiation Data Centre (WOUDC): http://www.woudc.org, https://doi.org/10.14287 /10000008. (last access: 04-11-2019). More information about the campaigns can be found at https://tropo.gsfc.nasa.gov/intexb/ions06. html, https://tropo.gsfc.nasa.gov/arcions/, and https://exp-studies. tor.ec.gc.ca/~bortas/.

Declaration of competing interest

The authors declare that they have no known competing financial interests or personal relationships that could have appeared to influence the work reported in this paper.

CRediT authorship contribution statement

Acknowledgements

Appendix A. Supplementary data

Supplementary data to this article can be found online at https://doi. org/10.1016/j.aeaoa.2020.100078.

References

Alvarado, M.J., Logan, J.A., Mao, J., Apel, E., Riemer, D., Blake, D., Cohen, R.C., Min, K. E., Perring, A.E., Browne, E.C., Wooldridge, P.J., Diskin, G.S., Sachse, G.W., Fuelberg, H., Sessions, W.R., Harrigan, D.L., Huey, G., Liao, J., Case-Hanks, A., Jimenez, J.L., Cubison, M.J., Vay, S.A., Weinheimer, A.J., Knapp, D.J., Montzka, D. D., Flocke, F.M., Pollack, I.B., Wennberg, P.O., Kurten, A., Crounse, J., Clair, J M St, Wisthaler, A., Mikoviny, T., Yantosca, R.M., Carouge, C.C., Le Sager, P., 2010.

Nitrogen oxides and PAN in plumes from boreal fires during ARCTAS-B and their impact on ozone: an integrated analysis of aircraft and satellite observations. Atmos. Chem. Phys. 10 (20), 9739–9760. https://doi.org/10.5194/acp-10-9739-2010.

Andreae, M.O., Anderson, B.E., Blake, D.R., Bradshaw, J.D., Collins, J.E., Gregory, G.L., Sachse, G.W., Shipham, M.C., 1994. Influence of plumes from biomass burning on atmospheric chemistry over the equatorial and tropical South Atlantic during CITE 3. J. Geophys. Res. 99 (D6), 12793–12808.

Andreae, M.O., Merlet, P., 2001. Emission of trace gases and aerosols from biomass burning. Glob. Biodeochemical Cycles 15 (4), 955–966.

Baylon, P., Jaffe, D.A., Wigder, N.L., Gao, H., Hee, J., 2015. Ozone enhancement in western US wild fire plumes at the Mt. Bachelor Observatory : the role of NOx, Atmos. Environ. Times 109 (x), 297–304. https://doi.org/10.1016/j. atmosenv.2014.09.013.

Bell, M.L., Zanobetti, A., Dominici, F., 2014. Who is more affected by ozone pollution? A systematic review and meta-analysis. Am. J. Epidemiol. 180 (1), 15–28. https://doi. org/10.1093/aje/kwu115.

Bourqui, M.S., Yamamoto, A., Tarasick, D., Moran, M.D., Beres, I., Davies, J., Elford, A., Hocking, W., Osman, M., Wilkinson, R., 2012. A new global real-time Lagrangian diagnostic system for stratosphere-troposphere exchange: evaluation during a balloon sonde campaign in eastern Canada. Atmos. Chem. Phys. 12 (5), 2661–2679. https://doi.org/10.5194/acp-12-2661-2012.

Busilacchio, M., Di Carlo, P., Aruffo, E., Biancofiore, F., Salisburgo, C.D., Giammaria, F., Bauguitte, S., Lee, J., Moller, S., Hopkins, J., Punjabi, S., Andrews, S., Lewis, A.C., Parrington, M., Palmer, P.I., Hyer, E., Wolfe, G.M., 2016. Production of peroxy nitrates in boreal biomass burning plumes over Canada during the BORTAS campaign. Atmos. Chem. Phys. 16 (5), 3485–3497. https://doi.org/10.5194/acp-16-3485-2016.

Canada's National Forestry Database, 2019. Forest Area Burned and Number of Forest Fires.

Charney, J.J., Bian, X., Potter, B.E., Heilman, W.E., 2003. The role of a stratospheric intrusion in the evolution of the Double State Park wildfire. In: Proceedings, 5th Symp. Fire for. Meteorol. Orlando, FL, 2002. Amer. Meteor. Soc.

Colette, A., Ancellet, G., 2005. Impact of vertical transport processes on the tropospheric ozone layering above Europe.: Part II: climatological analysis of the past 30 years. Atmos. Environ. 39 (29), 5423–5435. https://doi.org/10.1016/j. atmosenv.2005.06.015.

Cristofanelli, P., Bonasoni, P., Tositti, L., Bonafe, U., Calzolari, F., Evangelisti, F., Sandrini, S., Stohl, A., 2006. A 6-year analysis of stratospheric intrusions and their influence on ozone at Mt. Cimone (2165 m above sea level). J. Geophys. Res. 111 (3), 1–11. https://doi.org/10.1029/2005JD006553.

Downey, A., Jasper, J.D., Gras, J.J., Whittlestone, S., 1990. Lower tropospheric transport over the southern ocean. J. Atmos. Chem. 11 (1–2), 43–68. https://doi.org/10.1007/ BF00053667.

Draxler, R.R., Hess, G.D., 1998. An overview of the HYSPLIT_4 modelling system for trajectories, dispersion, and deposition. Aust. Meteorol. Mag. 47, 295–308.

Engström, a, Magnusson, L., 2009. Estimating trajectory uncertainties due to flow dependent errors in the atmospheric analysis. Atmos. Chem. Phys. 9, 8857–8867. https://doi.org/10.5194/acp-9-8857-2009.

Finch, D.P., Palmer, P.I., Parrington, M., 2014. Origin, variability and age of biomass burning plumes intercepted during BORTAS-B. Atmos. Chem. Phys. 14 (24), 13789–13800. https://doi.org/10.5194/acp-14-13789-2014.

Freitas, S.R., Longo, K.M., Chatfield, R., Latham, D., Dias, M.A.F.S., Andreae, M.O., Prins, E., Unesp, F.E.G., 2007. Including the sub-grid scale plume rise of vegetation fires in low resolution atmospheric transport models. Atmos. Chem. Phys. 7, 3385–3398.

Fromm, M.D., Servranckx, R., 2003. Transport of forest fire smoke above the tropopause by supercell convection. Geophys. Res. Lett. 30 (10), 1–4. https://doi.org/10.1029/ 2002GL016820.

Giglio, L., Descloitres, J., Justice, C.O., Kaufman, Y.J., 2003. An enhanced contextual fire detection algorithm for MODIS. Remote Sens. Environ. 87 (2–3), 273–282. https:// doi.org/10.1016/S0034-4257(03)00184-6.

Harris, J.M., Draxler, R.R., Oltmans, S.J., 2005. Trajectory model sensitivity to differences in input data and vertical transport method. J. Geophys. Res. Atmos. 110 (14), 1–8. https://doi.org/10.1029/2004JD005750.

Hocking, W.K., Carey-Smith, T., Tarasick, D.W., Argall, P.S., Strong, K., Rochon, Y., Zawadzki, I., Taylor, P. a, 2007. Detection of stratospheric ozone intrusions by windprofiler radars. Nature 450 (7167), 281–284. https://doi.org/10.1038/ nature06312.

Jacob, D.J., Heikes, B.G., Fan, S., Logan, J.A., Mauzerall, D.L., Singh, H.B., Gregory, G.L., Talbot, R.W., Blake, D.R., Et, J., Photochemistry, A.L., 1996. Origin of ozone and NOx in the tropical troposphere: a photochemical analysis of aircraft observations over the South Atlantic basin. J. Geophys. Res. Atmos. 101 (D19), 24235–24250.

Jaffe, D.A., Bertschi, I., Jaeglé, L., Novelli, P., Reid, J.S., Tanimoto, H., Vingarzan, R., Westphal, D.L., 2004. Long-range transport of Siberian biomass burning emissions and impact on surface ozone in western North America. Geophys. Res. Lett. 31 (16), 6–9. https://doi.org/10.1029/2004GL020093.

Jaffe, D.A., Wigder, N.L., 2012. Ozone production from wildfires: a critical review. Atmos. Environ. 51, 1–10. https://doi.org/10.1016/j.atmosenv.2011.11.063.

Kahn, R.A., Chen, Y., Nelson, D.L., Leung, F., Li, Q., Diner, D.J., Logan, J.A., 2008. Wildfire smoke injection heights : two perspectives from space. Geophys. Res. Lett. 35 (L04809), 1–4. https://doi.org/10.1029/2007GL032165.

Kaiser, J.W., Heil, A., Andreae, M.O., Benedetti, A., Chubarova, N., Jones, L., Morcrette, J., Razinger, M., 2012. Biomass burning emissions estimated with a global fire assimilation system based on observed fire radiative power. Bio Geosci 9, 527–554. https://doi.org/10.5194/bg-9-527-2012.

Kalnay, E., Kanamitsu, M., Kistler, R., Collins, W., Deaven, D., Gandin, L., Iredell, M., Saha, S., White, G., Woollen, J., Zhu, Y., Chellian, M., Ebisuzaki, W., Higgins, W., Janowiak, J., Mo, K.C., Ropelewski, C., Wang, J., Leetmaa, A., Reynolds, R., Jenne, R., Joseph, D., 1996. The NCEP/NCAR 40-year reanalysis project. Bull. Am. Meteorol. Soc. 77 (3), 437–471.

Labonne, M., 2007. Injection height of biomass burning aerosols as seen from a spaceborne lidar. Geophys. Res. Lett. 34 (L11806), 1–5. https://doi.org/10.1029/2007GL029311.

Langford, A.O., Pierce, R.B., Schultz, P.J., 2015. Stratospheric intrusions, the Santa Ana winds, and wildland fires in Southern California. Geophys. Res. Lett. 42 (14), 6091–6097. https://doi.org/10.1002/2015GL064964.

Lippmann, M., 1991. Health effects of tropospheric ozone. Environ. Sci. Technol. 25 (12), 1954–1962. https://doi.org/10.1021/es00180a002.

Liu, G., Liu, J., Tarasick, D.W., Fioletov, V.E., Jin, J.J., Moeini, O., Liu, X., Sioris, C.E., Osman, M., 2013a. A global tropospheric ozone climatology from trajectory-mapped ozone soundings. Atmos. Chem. Phys. 13 (21), 10659–10675. https://doi.org/10.5194/acp-13-10659-2013.

Liu, J., Tarasick, D.W., Fioletov, V.E., McLinden, C., Zhao, T., Gong, S., Sioris, C., Jin, J. J., Liu, G., Moeini, O., 2013b. A global ozone climatology from ozone soundings via trajectory mapping: a stratospheric perspective. Atmos. Chem. Phys. 13 (22), 11441–11464. https://doi.org/10.5194/acp-13-11441-2013.

MacDonald, A.M., Anlauf, K.G., Leaitch, W.R., Chan, E., Tarasick, D.W., 2011. Interannual variability of ozone and carbon monoxide at the Whistler high elevation site: 2002-2006. Atmos. Chem. Phys. 11 (22), 11431–11446. https://doi.org/10.5194/acp-11-11431-2011.

McConnell, R., Berhane, K., Gilliland, F., London, S.J., Islam, T., Gauderman, W.J., Avol, E., Margolis, H.G., Peters, J.M., 2002. Asthma in exercising children exposed to ozone: a cohort study. Lancet 359 (9304), 386–391. https://doi.org/10.1016/S0140-6736(02)07597-9.

Newell, R.E., Thouret, V., Cho, J.Y.N., Stoller, P., Marenco, A., Smit, H.G., 1999. Ubiquity of quasi-horizontal layers in the troposphere. Nature 398 (6725), 316–319. https://doi.org/10.1038/18642.

Olson, J.R., Crawford, J.H., Brune, W., Mao, J., Ren, X., Fried, A., Anderson, B., Apel, E., Beaver, M., Blake, D., Chen, G., Crounse, J., Dibb, J., Diskin, G., Hall, S.R., Huey, L. G., Knapp, D., Richter, D., Riemer, D., St Clair, J., Ullmann, K., Walega, J., Weibring, P., Weinheimer, A., Wennberg, P., Wisthaler, A., 2012. An analysis of fast photochemistry over high northern latitudes during spring and summer using in-situ observations from ARCTAS and TOPSE. Atmos. Chem. Phys. 12 (15), 6799–6825. https://doi.org/10.5194/acp-12-6799-2012.

Palmer, P.I., Parrington, M., Lee, J.D., Lewis, A.C., Rickard, A.R., Bernath, P.F., Duck, T. J., Waugh, D.L., Tarasick, D.W., et al., 2013. Quantifying the impact of BOReal forest fires on Tropospheric oxidants over the Atlantic using Aircraft and Satellites (BORTAS) experiment: design, execution and science overview. Atmos. Chem. Phys. 13 (13), 6239–6261. https://doi.org/10.5194/acp-13-6239-2013.

Parrington, M., Palmer, P.I., Henze, D.K., Tarasick, D.W., Hyer, E.J., Owen, R.C., Helmig, D., Clerbaux, C., Bowman, K.W., Deeter, M.N., Barratt, E.M., Coheur, P.F., Hurtmans, D., Jiang, Z., George, M., Worden, J.R., 2012. The influence of boreal biomass burning emissions on the distribution of tropospheric ozone over North America and the North Atlantic during 2010. Atmos. Chem. Phys. 12 (4), 2077–2098. https://doi.org/10.5194/acp-12-2077-2012.

Parrington, M., Palmer, P.I., Lewis, A.C., Lee, J.D., Rickard, A.R., Di Carlo, P., Taylor, J. W., Hopkins, J.R., Punjabi, S., Oram, D.E., Forster, G., Aruffo, E., Moller, S.J., Bauguitte, J.B.S., Allan, J.D., Coe, H., Leigh, R.J., 2013. Ozone photochemistry in boreal biomass burning plumes. Atmos. Chem. Phys. 13 (15), 7321–7341. https://doi.org/10.5194/acp-13-7321-2013.

Paugam, R., Wooster, M., Freitas, S., Martin, M.V., 2016. A review of approaches to estimate wildfire plume injection height within large-scale atmospheric chemical transport models. Atmos. Chem. Phys. 16, 907–925. https://doi.org/10.5194/acp-16-907-2016.

Pfister, G.G., Emmons, L.K., Hess, P.G., Honrath, R., Lamarque, J.F., Val Martin, M., Owen, R.C., Avery, M.A., Browell, E.V., Holloway, J.S., Nedelec, P., Purvis, R., Ryerson, T.B., Sachse, G.W., Schlager, H., 2006. Ozone production from the 2004 North American boreal fires. J. Geophys. Res. 111 (24), 1–13. https://doi.org/10.1029/2006JD007695.

Real, E., Law, K.S., Weinzierl, B., Fiebig, M., Petzold, A., Wild, O., Methven, J., Arnold, S. A., Stohl, A., Huntrieser, H., Roiger, A.E., Schlager, H., Stewart, D., Avery, M.A., Sachse, G.W., Browell, E.V., Ferrare, R.A., Blake, D., 2007. Processes influencing ozone levels in Alaskan forest fire plumes during long-range transport over the North Atlantic. J. Geophys. Res. Atmos. 112 (10), 1–19. https://doi.org/10.1029/2006JD007576.

Smit, H.G.J., Straeter, W., Johnson, B.J., Oltmans, S.J., Davies, J., Tarasick, D.W., Hoegger, B., Stubi, R., Schmidlin, F.J., Northam, T., Thompson, A.M., Witte, J.C., Boyd, I., Posny, F., 2007. Assessment of the performance of ECC-ozonesondes under quasi-flight conditions in the environmental simulation chamber: insights from the juelich ozone sonde intercomparison experiment (JOSIE). J. Geophys. Res. 112 (19), 1–18. https://doi.org/10.1029/2006JD007308.

Sofiev, M., Ermakova, T., Vankevich, R., 2012. Evaluation of the smoke-injection height from wild-land fires using remote-sensing data. Atmos. Chem. Phys. 12, 1995–2006. https://doi.org/10.5194/acp-12-1995-2012.

Spracklen, D.V., Mickley, L.J., Logan, J.A., Hudman, R.C., Yevich, R., Flannigan, M.D., Westerling, A.L., 2009. Impacts of climate change from 2000 to 2050 on wildfire activity and carbonaceous aerosol concentrations in the western United States. J. Geophys. Res. Atmos. 114 (20), 1–17. https://doi.org/10.1029/2008JD010966.

Stocks, B.J., Fosberg, M.A., Lynham, T.J., Mearns, L., Wotton, B.M., Yang, Q., Jin, J.Z., Lawrence, K., Hartley, G.R., Mason, J.A., McKenney, D.W., 1998. Climate change and forest fire potential in Russian and Canadian boreal forests. Climatic Change 38 (1), 1–13. https://doi.org/10.1023/A:1005306001055.

Stohl, A., 1998. Computation, accuracy and applications of trajectories-A review and bibliography. Atmos. Environ. 32 (6), 947–966. https://doi.org/10.1016/S1474-8177(02)80024-9.

Stohl, A., Spichtinger-Rakowsky, N., Bonasoni, P., Feldmann, H., Memmesheimer, M., Scheel, H.E., Trickl, T., Hübener, S., Ringer, W., Mandl, M., 2000. The influence of stratospheric intrusions on alpine ozone concentrations. Atmos. Environ. 34 (9), 1323–1354. https://doi.org/10.1016/S1352-2310(99)00320-9.

Szyszkowicz, M., Rowe, B.H., 2016. Respiratory Health Conditions and Ambient Ozone : A Case-Crossover Study Insights in Chest Diseases 1 (10), 155–161. https://doi.org/10.4137/EHI.S40493.

Tarasick, D.W., Carey-smith, T.K., Hocking, W.K., Moeini, O., He, H., Liu, J., Osman, M. K., Thompson, A.M., Johnson, B.J., Oltmans, S.J., Merrill, J.T., 2019c. Quantifying stratosphere-troposphere transport of ozone using balloon- borne ozonesondes , radar windprofilers and trajectory models. Atmos. Environ. 198, 496–509. https://doi.org/10.1016/j.atmosenv.2018.10.040.

Tarasick, D.W., Davies, J., Smit, H.G.J., Oltmans, S.J., 2016. A re-evaluated Canadian ozonesonde record : measurements of the vertical distribution of ozone over Canada from 1966 to 2013. Atmos. Meas. Tech. 9, 195–214. https://doi.org/10.5194/amt-9-195-2016.

Tarasick, D.W., Galbally, I., Cooper, O.R., Schultz, M.G., Ancellet, G., LeBlanc, T., Wallington, T.J., Ziemke, J., Liu, X., Steinbacher, M., Stähelin, J., Vigouroux, C., Hannigan, J.W., García, O., Foret, G., Zanis, P., Weatherhead, E., Petropavlovskikh, I., Worden, H., Osman, M., Liu, J., Chang, K.-L., Gaudel, A., Lin, M., Granados-Muñoz, M., Thompson, A.M., Oltmans, S.J., Cuesta, J., Dufour, G., Thouret, V., Hassler, B., Trickl, T., Neu, J.L., 2019. TOAR- Observations: tropospheric ozone observations from 1877 to 2017, measurement uncertainties and trends. Elem. Sci. Anthr. 7 (1), 39. http://doi.org/10.1525/elementa.376.

Tarasick, D.W., Jin, J.J., Fioletov, V.E., Liu, G., Thompson, A.M., Oltmans, S.J., Liu, J., Sioris, C.E., Liu, X., Cooper, O.R., Dann, T., Thouret, V., 2010. High-resolution tropospheric ozone fields for INTEX and ARCTAS from IONS ozonesondes. J. Geophys. Res. Atmos. 115 (20), 1–12. https://doi.org/10.1029/2009JD012918.

Tarasick, D.W., Smit, H.G.J., Thompson, A.M., Morris, G.A., Witte, J.C., Davies, J., Nakano, T., van Malderen, R., Stauffer, R.M., Deshler, T., Johnson, B.J., Stübi, R., Sterling, C., Oltmans, S.J., 2019b. Improving ECC ozonesonde data quality: assessment of current methods & outstanding issues. Earth Sp. Sci. Submitted for publication.

Teakles, A., So, R., Ainslie, B., Nissen, R., Schiller, C., Vingarzan, R., Macdonald, A.M., Jaffe, D.A., Bertram, A.K., Strawbridge, K.B., Leaitch, R., Hanna, S., Toom, D., Baik, J., Huang, L., 2016. Impacts of the july 2012 siberian fire plume on air quality in the pacific northwest. Atmos. Chem. Phys. Discuss. https://doi.org/10.5194/acp-2016-302.

Thompson, A.M., Oltmans, S.J., Tarasick, D.W., GathenVon Der, P., Smit, H G.J., Witte, J. C., 2011. Strategic ozone sounding networks : Review of design and accomplishments. Atmos. Environ. 45 (13), 2145–2163. https://doi.org/10.1016/j.atmosenv.2010.05.002.

Thompson, A.M., Pickering, K.E., Mcnamara, D.P., Schoeberl, M.R., Hudson, R.D., Kim, J.H., Browell, E.V., Kirchhoff, V.W.J.H., Nganga, D., 1996. Where did tropospheric ozone over southern Africa and the tropical Atlantic come from in October 1992? Insights from TOMS, GTE TRACE A, and SAFARI 1992. J. Geophys. Res. 101 (D19), 24251–24278.

Thompson, A.M., Stone, J.B., Witte, J.C., Miller, S.K., Pierce, R.B., Chatfield, R.B., Oltmans, S.J., Cooper, O.R., Loucks, A.L., Taubman, B.F., Johnson, B.J., Joseph, E., Kucsera, T.L., Merrill, J.T., Morris, G.A., Hersey, S., Forbes, G., Newchurch, M.J., Schmidlin, F.J., Tarasick, D.W., Thouret, V., Cammas, J.P., 2007a. Intercontinental chemical transport experiment ozonesonde network study (IONS) 2004: 1. Summertime upper troposphere/lower stratosphere ozone over northeastern north America. J. Geophys. Res. 112 (12), 1–15. https://doi.org/10.1029/2006JD007441.

Thompson, A.M., Witte, J.C., Hudson, R.D., Guo, H., Herman, J.R., Fujiwara, M., 2001. Tropical tropospheric ozone and biomass burning. Science 291, 2128–2133.

Thompson, A.M., Stone, J.B., Witte, J.C., Miller, S.k., Oltmans, S.J., Kucsera, T.L., Ross, K.L., Pickering, K.E., Merrill, J.T., Forbes, G., Tarasick, D.W., Joseph, E., Schmidlin, F.J., McMillan, W.W., Warner, J., Hintsa, E.J., Johnson, J.E., 2007b. Intercontinental Chemical Transport Experiment Ozonesonde Network Study (IONS) 2004: 2. Tropospheric ozone budgets and variability over northeastern North America. J. Geophys. Res 112 (D12). https://doi.org/10.1029/2006JD007670.

Val Martin, M., Honrath, R.E., Owen, R.C., Pfister, G., Fialho, P., Barata, F., 2006. Significant enhancements of nitrogen oxides , black carbon , and ozone in the North Atlantic lower free troposphere resulting from North American boreal wildfires. J. Geophys. 111 (D23S60), 1–17. https://doi.org/10.1029/2006JD007530.

Van Haver, P., De Muer, D., Beekmann, M., Mancier, C., 1996. Climatology of tropopause folds at midlatitudes. Geophys. Res. Lett. 23 (9), 1033–1036.

Vérèmes, H., Payen, G., Keckhut, P., Duflot, V., Baray, J.-L., Cammas, J.-P., Leclair De Bellevue, J., Evan, S., Posny, F., Gabarrot, F., Metzger, J.-M., Marquestaut, N., Meier, S., Vömel, H., Dirksen, R., 2017. A Raman lidar at Maïdo Observatory (Reunion Island) to measure water vapor in the troposphere and lower stratosphere: calibration and validation. Atmos. Meas. Tech. Discuss. (April), 1–38. https://doi.org/10.5194/amt-2017-32.

Verma, S., Worden, J., Pierre, B., Jones, D.B.A., Al-Saadi, J., Boersma, F., Bowman, K., Eldering, A., Fisher, B., Jourdain, L., Kulawik, S., Worden, H., 2009. Ozone production in boreal fire smoke plumes using observations from the Tropospheric Emission Spectrometer and the Ozone Monitoring Instrument. J. Geophys. Res. 114 (2) https://doi.org/10.1029/2008JD010108.

Weller, R., Lilischkis, R., Schrems, O., Neuber, R., Wessel, S., 1996. Vertical ozone distribution in the marine atmosphere over the central Atlantic Ocean (56S - 50N). J. Geophys. Res. 101 (D1), 1387–1399.

Wigder, N.L., Jaffe, D.A., Saketa, F.A., 2013. Ozone and particulate matter enhancements from regional wildfires observed at Mount Bachelor during 2004-2011. Atmos. Environ. 75, 24–31. https://doi.org/10.1016/j.atmosenv.2013.04.026.

WMO, 1957. A three-dimensional science: second session of the commission for aerology. WMO Bull 4 (2), 134–138.

Wotawa, G., Trainer, M., 2000. The influence of Canadian forest fires on pollutant concentrations in the United States. Science 288 (5464), 324–328. https://doi.org/10.1126/science.288.5464.324.

Wotton, B.M., Nock, C.A., Flannigan, M.D., 2010. Forest fire occurrence and climate change in Canada. Int. J. Wildland Fire 19, 253–271.

Zimet, T., Martin, J.E., Potter, B.E., 2007. The influence of an upper-level frontal zone on the Mack Lake Wildfire environment. Meteorol. Appl. 14 (January), 131–147. https://doi.org/10.1002/met.